

Source apportionment of ambient fine particulate matter in Dearborn, Michigan, using hourly resolved PM chemical composition data

Joseph Patrick Pancras^a, Matthew S. Landis^{b*}, Gary A. Norris^b, Ram Vedantham^b, J. Timothy Dvonch^c

^a*Alion Science and Technology, P.O. Box 12313, Research Triangle Park, North Carolina 27709*

^b*U.S. Environmental Protection Agency, Office of Research and Development, Research Triangle Park, North Carolina 27711*

^c*Department of Environmental Health Sciences, University of Michigan School of Public Health, Ann Arbor, MI, USA*

*Corresponding author phone: (919) 541-4841; e-mail: landis.matthew@epa.gov.

Abstract

High time-resolution aerosol sampling was conducted for one month during July-August 2007 in Dearborn, MI, a non-attainment area for fine particulate matter (PM_{2.5}) National Ambient Air Quality Standards (NAAQS). Measurements of more than 30 PM_{2.5} species were made using a suite of semi-continuous sampling and monitoring instruments. Dynamic variations in the sub-hourly concentrations of source ‘marker’ elements were observed when discrete plumes from local sources impacted the sampling site. Hourly averaged PM_{2.5} composition data for 639 samples were used to identify and apportion PM_{2.5} emission sources using the multivariate receptor modeling techniques EPA Positive Matrix Factorization (PMF) v4.2 and EPA Unmix v6.0. Source contribution estimates from PMF and Unmix were then evaluated using the Sustained Wind Instance Method (SWIM), which identified plausible source origins. Ten

sources were identified by both PMF and Unmix: (1) secondary sulfate, (2) secondary nitrate characterized by a significant diurnal trend, (3) iron and steel production, (4) a potassium-rich factor attributable to iron/steel slag waste processing, (5) a cadmium-rich factor attributable to incineration, (6) an oil refinery characterized by $La/Ce > 1$ specific to south wind, (7) oil combustion, (8) coal combustion, (9) motor vehicles, and (10) road dust enriched with organic carbon. While both models apportioned secondary sulfate, oil refinery, and oil combustion $PM_{2.5}$ masses closely, the mobile and industrial source apportionments differed. Analyses were also carried out to help infer time-of-day variations in the contributions of local sources.

Keywords: High time-resolution measurements, trace elements, sulfate, nitrate, $PM_{2.5}$, source apportionment, Unmix, PMF

1. Introduction

Seven counties in southeastern Michigan were deemed non-attainment areas of the National Ambient Air Quality Standards (NAAQS) for fine particulate matter ($PM_{2.5}$) (NAAQS 2006; U.S. EPA, 2011a). Local county, state, and federal air quality regulatory agencies conducted several monitoring and technical studies on the nature of $PM_{2.5}$ violations in this region (Brown et al., 2006; Hammond et al., 2008; Wade et al., 2007). These studies found that secondary sulfate and local traffic were contributing 60–80% of the measured $PM_{2.5}$. All of the aforementioned studies used Federal Reference Method (FRM) 24 h integrated PM filter media based samples for analysis. This widely used approach does not have sufficient time resolution to quantify the impact of short-lived (quickly varying) emission events as can occur in non-continuous industrial processes such as steel making, or plume impact events that occur due to

transient meteorological conditions. Measurement of PM constituents at the same time scale of industrial processes and meteorological variability (< 1 hour) is an important step for understanding aerosol behavior and supporting source apportionment studies.

Measurements can be made on the time scale of dynamic atmospheric processes, such as wind direction shifts, that affect atmospheric aerosol concentrations (Pancras et al., 2006, 2011). Such time-resolved PM_{2.5} composition measurements can also help uncover epidemiological associations between short-term pollution concentrations and health effects (Ondov et al., 2006; Dockery and Pope, 1994; Wichmann et al., 2000). For example, Williams et al. (2012) found daily potassium air concentrations to be associated with decreased diastolic blood pressure in Detroit, MI. Mitcus (2004) reported that increased short-term concentrations of zinc played a role in stimulating respiratory cells to produce cytokines and reactive oxygen species.

Recently, Morishita et al. (2011) conducted a sub-hourly PM_{2.5} characterization study in the southwest Detroit area (Maybury Elementary School) and were able to identify six sources: secondary aerosol, motor vehicles, iron and steel production, oil refining, incineration, and cement/lime production. This study, however, did not report diurnal characteristics, typically resolvable, in high time-resolution measurements. In another study conducted in the Allen Park neighborhood in southwest Detroit, 3 h integrated PM_{2.5} measurements revealed nine sources, including four sulfur factors (Pere-Trepat et al., 2007). PM_{2.5} apportionment was not attempted in this study, and anions and carbon data were also not reported.

This study aimed to use high time-resolution PM_{2.5} composition measurements to assess the characteristics of local sources and to quantify their impact on local air pollution. In contrast to other studies in which receptor models have been applied on 24 h integrated samples that necessitated long-term collection over years to collect the necessary number of samples for a

robust numerical analysis, this study was able to accomplish this goal by using a relatively small data collection period (4 weeks). Multivariate receptor models (MRMs), EPA Positive Matrix Factorization (PMF) v4.2 and EPA Unmix v6.0, were applied on the collected data to identify and apportion PM emission sources. The Unmix model had been found suitable for high time-resolution data sets in one of our earlier studies (Pancras et al., 2011). PMF is another widely used MRM that uses the time variance of PM species concentrations at the receptor, and the correlations among species, to estimate the time variance of contributions and contributing source signatures at the measurement site (Hopke, 2003; U.S. EPA, 2011b). This model, however, requires information on uncertainties in the measurements of pollutant load. Incorrect error estimates can play a significant role in the modeling outcome (Reff et al., 2007). For this reason, two modified third-generation Semi-continuous Elements in Aerosol Sampler (SEAS-III) instruments were collocated in Dearborn, MI, and operated continuously throughout the study period. The work presented in this manuscript uses whole-system precision estimates from the collocated concentration measurements (Pancras and Landis, 2011). The Sustained Wind Incidence Method (SWIM) (Vedantham et al., 2012) was then applied to identify and estimate contributions from local point sources in this study.

2. Experimental methods

2.1 Receptor site

The Dearborn receptor site was an existing Chemical Speciation and Trends Network (CSTN) site located in the industrial core of southeast Detroit, MI (42.3075 N, 83.1496 W). A variety of potential NO_x, SO₂, and primary PM_{2.5} emission sources are present within a 10 km radius of the site (Fig. 1). The sources include metallurgical coke production, iron and steel

production, slag processing, oil refining, electric power generation, automobile manufacturing, metals recycling, incineration, and construction materials facilities. In addition to point sources, nearby highway traffic, heavy-duty truck depots, and service railroad traffic also contribute to the air pollution.

During this sampling campaign, the daily (95th percentile of daily average mass as defined in NAAQS, 2006) and monthly average PM_{2.5} mass concentrations were 39 $\mu\text{g m}^{-3}$ and 15.7 $\mu\text{g m}^{-3}$, respectively. Both observations are in exceedance of the respective NAAQS values of 35 $\mu\text{g m}^{-3}$ (daily) and 15 $\mu\text{g m}^{-3}$ (annual).

2.2 *Field measurements*

The U.S. Environmental Protection Agency (EPA) modified Semi-continuous Elements in Aerosol Sampler III (SEAS-III, Ondov Enterprises Inc., Clarksville, MD) collected aerosol samples at 30 min intervals for a total of 29 days in July and August 2007. The collected samples were analyzed for trace elements by high-resolution magnetic sector field inductively coupled plasma mass spectroscopy (HR-ICPMS). The modifications made to the standard SEAS-III and its field operation conditions, as well as the chemical analysis of the collected samples, are described in an earlier paper (Pancras and Landis, 2011). Briefly, the original inlet impactor was replaced with a Teflon-coated cyclone inlet (URG-2000-30ENB, URG Corp., Chapel Hill, NC) and the inlet steam manifold was redesigned to provide improved steam injection characteristics before undergoing heterogeneous condensational growth in the condenser column.

Real-time, semi-continuous (hourly) PM_{2.5} nitrate and sulfate measurements were carried out using a URG Corp (Chapel Hill, NC) Model 9000D Ambient Ion Monitor (AIM). Hourly PM_{2.5} mass concentration data were measured using a Thermo Fisher Scientific (Franklin, MA)

Model 1400A tapered-element oscillating microbalance (TEOM) instrument. A Sunset Laboratory Inc (Tigard, OR) Model 3 semi-continuous elemental and organic carbon (EC-OC) field analyzer was used to quantify EC and OC at an hourly resolution. Ambient concentrations of NO_x, SO₂, and CO were continuously measured at 1 min intervals using Thermo Environmental (Franklin, MA) models 42CTL, 43CTL, and 48CTL, respectively. Elemental gaseous mercury (GEM), divalent reactive gaseous mercury (RGM), and particulate bound mercury (Hg(p)) were measured at hourly resolution using two Tekran Instrument Corporation (Knoxville, TN) speciation systems (models 2537A, 1130, 1135) running asynchronously (Landis et al., 2002). Meteorological data, including wind direction and speed (10 m above ground level), were also measured at 1 min time intervals using an RM Young (Traverse City, MI) model 05305V-AQ wind monitor. The diurnal variations in atmospheric boundary layer mixing depths were obtained from the NOAA Air Resources Laboratory Web server (NOAA, 2012).

2.3 *Data analysis*

Mean hourly SEAS trace element, SO₂, NO_x, CO, and meteorological data were calculated for modeling purposes since PM_{2.5}, EC, OC, nitrate, and sulfate ion measurements were made hourly. Data quality control checks such as comparison of reconstructed PM_{2.5} mass to measured PM_{2.5} mass and comparison of filter-based sulfate to AIM sulfate concentrations were performed prior to source apportionment. Samples where reconstructed mass exceeded the measured PM_{2.5} mass by 30% were invalidated. Those sampling intervals for which all trace elements were missing were also invalidated (Pancras and Landis, 2011). Overall, approximately 5% of the collected data did not meet the aforementioned QA performance criteria and hence were excluded from the data analysis.

2.4 *PM mass reconstruction*

Hourly PM_{2.5} measurement data were validated by comparing 12 h average concentrations with the PM_{2.5} mass data obtained by an equivalent FRM. Ordinary least squares linear regression (OLS) analysis resulted in a slope of 0.96 and a coefficient of determination (r^2) of 0.93. PM_{2.5} mass concentration was then reconstructed at an hourly resolution from the available chemical speciation data. Contributions from trace metal oxide components were calculated after multiplying each element concentration by an appropriate factor to account for the oxygen associated with these elements (Cheung et al., 2011). Organic mass (OM) contribution was obtained by multiplying the measured OC by a factor of 1.6 (Turpin and Lim, 2001). Secondary aerosol contribution was estimated using AIM sulfate and nitrate concentration measurements (counter ions were assumed to be ammonium).

2.5 *Data modeling*

EPA PMF v4.2 and EPA Unmix v6.0 models were used for receptor modeling. The *EPA PMF 4.2 Fundamentals & User Guide* (U.S. EPA, 2011b) and *EPA Unmix 6.0 Fundamentals User Guide* (U.S. EPA, 2007) were followed to optimize model run conditions.

The EPA PMF allows users to down-weight any species concentration measurement on the basis of signal-to-noise ratio, and *a priori* knowledge of sampling/analytical issues. By setting a species ‘weak’ in the PMF program, its uncertainty is tripled for modeling purposes. In this work, Al and P concentrations were set to “weak” because of their poor analytical extraction efficiency (Pancras and Landis, 2011). Gaseous species were also set as “weak”. Method detection limits (MDLs) and precision estimates for PM_{2.5}, anions, trace elements, and carbon fractions used in our modeling effort are shown in Table 1. Uncertainty for PMF analysis was

estimated from MDL and precision estimate (error fraction) values using equation 1 (U.S. EPA, 2011b):

$$\text{Uncertainty} = \sqrt{(\text{error fraction} \times \text{concentration})^2 + \text{MDL}^2} \quad (1)$$

If the concentration was less than or equal to the MDL provided, the uncertainty was calculated using equation 2 (Polissar et al., 1998; U.S. EPA, 2011b):

$$\text{Uncertainty} = 5/6 \times \text{MDL} \quad (2)$$

No extra modeling uncertainty was used. Block bootstrapping (BBS), a non-parametric statistical tool, was used to estimate variability or modeling uncertainty in the source contribution estimates (U.S. EPA, 2011b). The BBS method captures effects from random errors in the solution, and also partially accounts for errors from computational rotational ambiguity.

SWIM sector apportionment was used to determine the percentage of the mean concentration or contribution that could be attributed to a wind sector that was preselected based on the location of known sources. SWIM uses surface meteorology data along with either the concentration data or source contributions to identify contributing transport sectors (Vedantham et al., 2012). Diurnal trends in the species and source contribution estimates (SCEs) were explored by constructing time-of-day contribution plots and box plots. The 3D contour plots were generated in SigmaPlot v12.3 (Systat Software Inc., Chicago, IL).

3. Results and discussion

3.1 Mass closure analysis

PM_{2.5} mass concentrations were reconstructed on an hourly basis from the available chemical speciation data (refer to section 2.4). Organic matter accounted for 50% of the reconstructed PM mass. Ammonium sulfate, ammonium nitrate, and EC accounted for 34%, 7%,

and 5% of the mass, respectively. Metal oxides contributed up to 4% of the mass. OLS regression analysis showed an r^2 of 0.89 and a slope of 0.82 ± 0.10 at a 95% confidence interval (CI). The mass fraction that was unaccounted for may be attributable to a combination of measurement and conversion factor errors used in this mass closure analysis.

3.2 HAP measurements

This study acquired semi-continuous concentrations of nine hazardous air pollutants (HAPs; Sb, As, Cd, Co, Pb, Mn, Hg, Ni, and Se) whose ambient concentrations will soon be regulated by the U.S. EPA Utility Air Toxics Rule (U.S. EPA, 2011c). At times, atmospheric concentrations of Sb, As, Cd, Pb, Mn, and Hg were at least 10-100 times higher than their respective background concentrations when discrete plume events from local sources impacted the receptor site (Table 2). For instance, high Mn levels were frequently observed from upwind events in the 210–260 degree wind sector (Fig. 2A). The SWIM sector apportionment results show that 49% of the observed mean Mn concentration was transported to the receptor by winds from 210–260 degrees. This result indicates that the average ambient concentration of Mn could be reduced up to 49% by controlling emissions from one local industrial operation(s) that lies in this wind direction.

Mercury is one of the most toxic HAPs released from industrial processes such as power generation. Unlike GEM, RGM and Hg(p) are soluble resulting in near field deposition gradients and can pose more environmental health issues (U.S. EPA, 1997). RGM and Hg(p) were observed predominantly during the period when winds were from the south and southwest, respectively (Fig. 2B and C), while GEM emissions were noted from multiple areas at moderately elevated levels (Fig. 2D). The combination of high time resolution measurements and the application of the SWIM model as demonstrated here can provide information on the

location of emission sources that may be helpful for policy makers and compliance authorities in regulating HAP emissions, where applicable.

3.3 *PMF receptor modeling*

In this study, the PMF model was found to produce a 10-factor solution with good bootstrap error estimation diagnostics. All 30 species included in the model (PM_{2.5}, OC, EC, sulfate, nitrate, SO₂, NO_x, CO, Al, As, Ba, Ca, Cd, Ce, Cu, Fe, K, La, Mg, Mn, Na, Ni, P, Pb, Rb, Se, Sr, Ti, V, and Zn) explained 88% of the total variance in the input data. A total of 16 species (PM_{2.5}, nitrate, sulfate, As, Ba, Ca, Cd, Ce, Fe, K, La, Mn, Rb, Se, Ti, and V) showed predicted versus observed concentrations with an $r^2 > 0.7$ and slope > 0.7 . Fit statistics for some key tracer species (Pb, Sr, Cd, Ni) were poor ($r^2 = 0.6-0.4$ and slope = $0.6-0.3$). Time-series concentration analysis showed that sharp concentration events in the observed Pb and Sr concentrations were largely under predicted by the model. PMF factor profiles are shown in Fig. 3.

The PMF solution was further evaluated using BBS to determine the error estimates associated with the factor profiles. Results showed instability between the Fluid Catalytic Cracking (FCC) and crustal factor profiles. Both of these profiles have significant La and Ce contributions, and the creation of the datasets for the BBS analysis may have missed the transient FCC peaks but still capture the more stable crustal contributions. This may explain the instability in the BBS results as seen in time-series analysis of the FCC source contributions. La and Ce concentrations were further evaluated with SWIM to determine if they were associated with a known source location or if the results were a mathematical artifact. The FCC La and Ce influences were limited to a very small wind quadrant (160–180 degrees) and the 155-190 degree domain consists of petroleum cracking facilities just a short distance away from the receptor site.

Thus, in spite of the BBS results, the FCC factor profile is very unlikely to be a mathematical artifact.

3.3.1 Source assignments

Arsenic is the single largest contributor to factor 1 with 65% of its modeled concentration attributed to this source. The other significant trace components of this factor NO_x (36%), EC (13%), OC (15%) and P (16%) suggest a motor vehicle source (Landis et al., 2007). Time-of-day analysis of the SCEs showed daily maximum between late night and early morning (Fig. 4A). No significant ($\alpha=0.05$) difference was observed between weekday and weekend trends. The atmospheric mixed layer depth at hourly resolution during the study period (Fig. 5B) shows the lowest mixing height at the site between late evening and early morning. The observed inverse relationship between SCE and mixing height implies a ground level emission source. There are several truck depots less than 2 km north and northwest of the receptor site. The SWIM plot of SCEs (Fig 6A) depicts the contribution from these wind sectors. A large number of idling motor vehicles (predominantly heavy duty trucks) and trains were observed throughout the night in the vicinity of the study area.

A box plot was constructed to examine if the major contributor of this factor, arsenic, displayed similar time-of-day behavior. Indeed, the measured arsenic concentrations exhibited a clear nighttime to early morning maxima (Fig. 5A), during which the mixing height was correspondingly low. Studies by Talebi and Abedi (2005) and Balakrishna et al. (2011) have associated arsenic with road-traffic emissions. Our measurement data and modeling effort, as elucidated above, also compel us to attribute this factor to motor vehicles emission.

With 79% of the modeled concentration, Se constituted a majority of Factor 2, which indicates a source related to coal combustion (Thurston and Spengler, 1985, Ondov and Wexler,

1998, Keeler et al., 2006). The SWIM plot of SCE (Fig. 6B) attributes one-third of the emissions to a small wind quadrant at 140–180 degrees. Zug Island lies within this sector, which contains an integrated iron and steel facility that includes coke batteries that use coal to make metallurgical coke. Metallurgical coke is a critical reducing agent used in the smelting of raw ore into iron. The SWIM plots of raw SO₂ concentrations (Fig. 6-K), also emitted from coke production, shows a similar contribution pattern from the 140–180 degree wind sector. Mn and Fe concentrations in this factor were not elevated enough to be considered primary iron/steel mill emissions. Coking is a major industrial process that emits volatile elements such as Se, As, Pb, SO₂, and RGM (Konieczynski et al. 2012). Hourly measured RGM concentrations were elevated, up to 200 pg m⁻³, when winds came from this wind quadrant (Fig. 2B). Therefore, we attribute this factor to metallurgical coke production.

Major species such as Ca (68%), Mg (62%), Sr (58%), Al (41%), Ti (41%), along with OC (31%) and EC (22%) characterize Factor 3. Time-of-day analysis established contribution estimates for this factor peaking in the morning (07:00–08:00) and remaining elevated for the duration of a typical work day (Fig. 4B). Weekday and weekend emission patterns are similar but with reduced strengths, suggesting a direct association with vehicle volume counts on weekdays and weekends. The SWIM plot shows contributions from all wind sectors (Fig. 6C) supporting the assignment of a non-stationary source. Since this factor is rich in crustal elements, it likely represents a mix of tailpipe emissions and resuspended road dust contributions (Landis et al., 2012).

The presence of V, Ni, and La, with La/V < 0.02 indicates Factor 4 is an oil combustion source (Ondov and Wexler, 1998; Kulkarni et al., 2007). Source contribution analysis by SWIM attributes 45% of this factor contribution to the 0-90 degree wind quadrant (Fig. 6D). No known

major commercial or industrial utility boilers that burn #2 or #6 oil are near the Dearborn site except one major electric utility (at ~ 130 degrees), which had reportedly ceased its oil burning operation at the time of this study. However, it is not uncommon for small- to medium-scale industries to use oil-fired boilers for their steam/energy needs.

Species such as La and Ce at a ratio greater than 1 in Factor 5 suggests the presence of fluid catalytic cracking (FCC) emissions from an oil refinery (Kulkarni et al., 2007). All other trace elements show insignificant loading in this factor, as the FCC emissions are primarily organic matter. The SWIM sector analysis estimates 60% of factor contributions come from the 155–195 degree wind sector (Fig. 6E). An oil refinery located 3 km south of the receptor site is likely responsible for this factor.

Factor 6 contains 80% nitrate and 38% EC. The diurnal plot shows nighttime maxima extending into morning traffic hours (Fig. 4D). Contributions tend to decrease after 12:00. A rise in temperature during the day most likely decomposed particle-phase nitrate to gas-phase nitrogen oxides. A significant drop in contribution during weekends also coincides with a drop in weekend NO_x concentrations (Fig. 4E). This factor is therefore ascribed to secondary nitrate aerosol.

Factor 7 is characterized by the presence of Cd (91%), along with contributions from Pb, Cu and Zn at concentration ratios of 1:2 and 1:10, respectively. Sharp Cd excursions on a time scale lasting up to 4 hours and specific to eastern winds suggested that this factor represents a local source. The sector apportionment plot (Fig. 6G) confirms the local source assignment. It attributes 65% of the total emissions to the 30-170 degree wind quadrant. A municipal incinerator (10.5 km at a bearing of 50 degrees) and a solid waste sludge incinerator (3.2 km at a bearing of 143 degrees) were the likely the sources of this factor. A tall tree within 50 m

northeast of the sampling site may have affected the reliability of wind measurements and might have affected the sector assignment.

Factor 8 consists largely of sulfate (80%), but also contains OC (37%) and EC (16%). Most sulfate aerosol in the atmosphere comes from the photochemical conversion of SO₂ (Seinfeld and Pandis, 1998). Sulfate is typically considered to be a regional pollutant in the Midwest due to its proximity with the Ohio River Valley's high density of coal-fired utility boilers. However, the SWIM plot of the SCE for this factor (Fig. 6H) show significant contributions from the 140-180 and 260-280 degree wind sectors, suggesting local combustion sources play a significant role in PM_{2.5} sulfate in this airshed. Time-of-day analysis showed no significant diurnal variability (Fig. 4C).

The characteristic species of Factor 9 are Fe, Mn, Pb, Cu, and Zn. These elements are typically found in fine particles from iron and steel manufacturing industries (Jiug-Horng et al., 2007). The sector apportionment results show 42% of the emissions are specific to wind angle 210–260 degrees (Fig. 6I). An iron and steel production facility is located in this wind quadrant less than 1 km from the receptor site.

Factor 10 consists of K, Mn, Rb, and Fe. Approximately 57% of K is attributed to this factor. Time-series concentrations and the SWIM plot of SCE point to a source of origin at approximately 210 degrees (Fig. 6J). Impacts from this factor were observed at the receptor site mostly during periods of medium to high wind speeds, suggesting that wind-blown fugitive dust was a likely source. Slag sintering plants are reported to emit large quantities of K (Jiun-Horng et al., 2007; Oravisjarvi et al., 2003; Dall'Osto et al., 2008). An iron and steel waste oxides reclamation facility is located to the southwest of the monitoring site (Fig. 1) and was identified

by SWIM as the source. Therefore, we attribute this factor to metals recovery slag processing. The proximity of the source could explain the smearing of the contributions in the SWIM plot.

3.4 *Unmix modeling*

Unmix also produced a similar 10-factor solution using much fewer species: PM_{2.5}, OC, EC, SO₄, NO₃, SO₂, NO_x, CO, As, Ca, Cd, Ce, Cu, Fe, K, La, Mg, Rb, Se, and V. Unlike PMF, Unmix is not designed to produce a feasible solution for any combination of species and for any number of factors. Only those species that help create a suitable hyperspace can be used in Unmix. The dimension of hyperspace is related to the number of requested factors. Thus, using a trial and error method, the abovementioned species were found to be a good combination that not only produced a robust feasible solution, but also that was highly interpretable. On the basis of trace elemental composition patterns, most of the Unmix factors were found to be similar to the factors identified by using PMF. Except for the coal combustion related factor, all other Unmix factor profiles were characterized by the same set of species as in PMF profiles and therefore are not discussed here. The coal combustion profile of Unmix comprised 70% SO₂ whereas the PMF generated profile was dominated by Se. Other differences include the percent of species strongly associated with the factors. The iron and steel factor accounted for 73% of the modeled Fe, which is 26% higher than the PMF profile loading. Also, the Unmix model identified mobile source factor appears to be influenced by re-suspended road dust (highlighted by about 27% of Ca, a byproduct of the slag operations from nearby facilities). Similarly, the crustal profile generated by PMF appears to be contaminated by the presence of OC (31%). Fit statistics from Unmix were robust with Pearson regression value of 0.80 or above for all species except NO_x (0.74), As (0.75), and OC (0.77).

Unmix factors were paired with PMF factors, and linear regression analysis was performed between the pairs of Unmix and PMF factor contribution estimates. As shown in Table 3, seven sources showed good agreement between the two model results ($r^2 > \sim 0.6$, slope $> \sim 0.7$). The disagreement in the motor vehicle and resuspended road dust factors is most likely a result of insufficient resolution of these sources by either of the models.

3.5 *PM apportionment*

Table 4 presents the PM_{2.5} mass apportioned to each source by both modeling approaches. The measured average PM_{2.5} mass was 15.6 $\mu\text{g m}^{-3}$. Unmix had better agreement with measured mass (15.4 $\mu\text{g.m}^{-3}$) than PMF, which explained 13.8 $\mu\text{g m}^{-3}$, meaning that 1.8 $\mu\text{g m}^{-3}$ of the measured PM_{2.5} mass in the PMF model was not accounted for by any of the sources. Both model estimates were similar for the contribution of secondary sulfate, and oil combustion sources to PM_{2.5} mass. The low agreement between the Unmix and PMF Iron and Steel, Crustal/Road Dust, Secondary Nitrate/Selenium factors suggests that the contributions should be interpreted with caution and supplementary methods such as microscopy for the metal and crustal sources might help differentiate their contributions (also see Table 3). Both Unmix and PMF estimated negligible amounts of PM_{2.5} mass attributable to refinery and coal/coke sources.

Table 4 also includes PM_{2.5} mass apportionment results from prior studies conducted at the Dearborn site that used FRM filter-based sampling techniques. Secondary sulfate mass from this study is similar to that found in previous studies. Earlier studies reported a mixed industrial factor driven by Zn and Pb concentrations. The Pb and Zn are associated with steel production in our analysis. The Iron/Steel contribution may be lower than previous studies due to the Severstal steel plant blast furnace (located across the street from the monitoring site) being shut down for maintenance during this study.

4. Summary

Both PMF and Unmix produced comparable factor compositions and contribution estimates for seven factors: incineration, secondary nitrate, coal/coke, oil combustion, sinter/slag processing, refining, and secondary sulfate. Both models found iron and steel sources and motor vehicle sources with slightly varying contribution estimates. SWIM convincingly identified plausible local sources based on modeled SCEs. Secondary sulfate aerosol mass from this study compares well with earlier reports. Although this data set is a rich source of information on inorganic PM constituents, it was limited by its lack of information on organic tracer species specific to mobile sources. Therefore, both models differed somewhat in apportioning PM mass to mobile sources.

Some local point sources did not appear to contribute significant $PM_{2.5}$ to the site. However, local point sources were found to contribute significantly higher concentrations of HAP elements Mn, Cd, Pb, and Hg. Hourly data also revealed a separate potassium-rich emission point source in this study region, which in earlier studies was thought to originate from traffic-related activity.

The collection and analysis of high time resolution $PM_{2.5}$ data allowed for the following improvements over 24 h integrated sampling: (i) all of the source categories found from earlier studies that used filter-based sampling and long sample collection periods (several years) were confirmed in only 4 weeks of sample collection, (ii) time of day analysis could be used to confirm the factor identification based on traffic counts or production schedules, and (iii) the application of SWIM to the high time resolution $PM_{2.5}$ data allowed for the identification of specific facility locations impacting the site rather than just source categories as typically reported when using 24 h integrated filter data. In cases where the $PM_{2.5}$ source mix is expected

to change with season (e.g., winter season home heating, summer season forest fires) additional seasonal monitoring intensives would be needed to characterize the annualized source contributions.

Acknowledgments

The U.S. Environmental Protection Agency (EPA) through its Office of Research and Development funded, managed, and participated in the research described here under (i) contract EP-D-10-070 with Alion Science and Technology, and (ii) contract RD83479701 with the University of Michigan Air Quality Laboratory. The views expressed in this paper are those of the authors and do not necessarily reflect the views or policies of EPA. It has been subjected to EPA Agency review and approved for publication. Mention of trade names or commercial products does not constitute endorsement or recommendation for use.

The authors thank Russell Long of EPA's National Exposure Research Laboratory for providing the URG AIM data and the Michigan Department of Environmental Quality for access to the monitoring site and for providing TEOM and OC/EC data. We would also like to thank Shelly Eberly of Sonoma Technology, Inc., and Pentti Paatero of the University of Helsinki, Finland, for their helpful PMF-related comments, and Stacy Henkle of Alion Science and Technology for technical editing of the manuscript.

References

- Balalrishna, G, Pervez, S, Bisht, DS. Source apportionment of arsenic in atmospheric dust fall out in an urban residential area, Raipur, Central India. *Atmos. Chem. Phys.* 2011; 11: 5141-5151.
- Brown SG, Hafner HR, Roberts PT, Schauer JJ, Sheesley RJ. Integration of Results for the Upper Midwest Urban Organics Study, Report STI-903520-2942-FR, Sonoma Technology, Inc., Chicago, IL, 2006.
- Cheung K, Daher N, Kam W, Shafer MM, Ninga Z, Schauer JJ, Sioutas C. Spatial and temporal variation of chemical composition and mass closure of ambient coarse particulate matter (PM_{10-2.5}) in the Los Angeles area. *Atmos Environ* 2011;45:2651–62.
- Dall'Osto M, Booth MJ, Smith W, Fisher R, Harrison RM. A study of the size distributions and the chemical characterization of airborne particles in the vicinity of a large integrated steelworks. *Aerosol Sci Technol* 2008;42: 981–91.
- Dockery DW, Pope CA. Acute respiratory effects of particulate air pollution. *Ann Rev Public Health* 1994;15:107–32.
- Gildemeister AE, Hopke PK, Kim E. Sources of fine urban particulate matter in Detroit, MI. *Chemosphere* 2007;69;1064–74.
- Hammond DM, Dvonch JT, Keeler GJ, Parker EA, Kamal AS, Barres JA, Yip FY, Brakefield-Caldwell W. Sources of ambient fine particulate matter at two community sites in Detroit, Michigan. *Atmos Environ* 2008;42:720–32.
- Hopke PK. Recent developments in receptor modeling. *J Chemom* 2003;17:255–65.

- Jiun-Horng T, Kuo-Hsiung L, Chih-Yu C, Jian-Yuan D , Ching-Guan C , Hung-Lung C.
Chemical constituents in particulate emissions from an integrated iron and steel facility. *J Hazard Mater* 2007;147:111–19.
- Keeler, G.J., Landis, M.S., Norris, G.A., Christianson, E.M., Dvonch, J.T. Sources of mercury wet deposition in eastern Ohio, USA. *Environ. Sci. Technol.* 2006; 40: 5874-5881.
- Konieczynski, J., Zajusz-Zubek, E., Jabonska, M. The Release of Trace Elements in the Process of Coal Coking. *The Scientific World Journal*, 2012 (DOI:10.1100/2012/294927).
- Kulkarni P, Chellam S, Fraser MP. Tracking petroleum refinery emission events using lanthanum and lanthanides as elemental markers for PM_{2.5}. *Environ Sci Technol* 2007;41:6748–54.
- Landis MS, Stevens RK, Schaedlich F, Prestbo E. Development and characterization of an annular denuder methodology for the measurement of divalent inorganic reactive gaseous mercury in ambient air. *Environ Sci Technol* 2002;36:3000–9.
- Landis, M.S., Lewis, C.W., Stevens, R.K., Keeler, G.J., Dvonch, T., Tremblay, R. Ft. McHenry Tunnel Study: Source Profiles and Mercury Emissions from Diesel and Gasoline Powered Vehicles. *Atmos Environ.* 2007; 41: 8711-8724.
- Landis, M.S., Pancras, J.P., Graney, J.R., Stevens, R.K., Percy, K.E., Krupa, S. Receptor Modeling of Epiphytic Lichens to Elucidate the Sources and Spatial Distribution of Inorganic Air Pollution in the Athabasca Oil Sands Region. In *Alberta Oil Sands: Energy, Industry and the Environment*, 2012. Kevin Percy ed., Elsevier, Oxford, England.
- Mitcus R. Analysis of the role of zinc, a major component of ambient Baltimore fine particle matter, in eliciting cytokine and chemokine release and disrupting cellular tight junctions in vitro. Ph.D. Dissertation, University of Maryland, Baltimore County, MD, 2004.

- Morishita M, Keeler GJ, Kamal AS, Wagner FG, Harkema JR, Rohr AC. Identification of ambient PM_{2.5} sources and analysis of pollution episodes in Detroit, Michigan using highly time-resolved measurements. *Atmos Environ* 2011;45:1627–37.
- National Ambient Air Quality Standards for Particulate Matter, Final Rule, *Federal Register*, October 17, 2006: 71 FR 61165–61167.
- National Oceanic and Atmospheric Administration (NOAA) Air Resources Laboratory (ARL), Archived Meteorological Products, NOAA ARL, Silver Spring, MD, <http://www.arl.noaa.gov/ready/amet.html>, last accessed February 9, 2012.
- Ondov JM, Wexler AS. Where do particulate toxins reside? An improved paradigm for the structure and dynamics of the urban mid-Atlantic aerosol. *Environ Sci Technol* 1998;32:2547–55.
- Ondov JM, Buckley TJ, Hopke PK, Ogulei D, Parlange MB, Roggee WF, Squibb KS, Johnston MV, Wexler AS. Baltimore Supersite: highly time- and size-resolved concentrations of urban PM_{2.5} and its constituents for resolution of sources and immune responses. *Atmos Environ* 2006;40:S224–37.
- Oravisjarvi K, Timonen KL, Wiikinkoski T, Ruuskanen AR, Heinanen K, Ruuskanen J. Source contribution to PM_{2.5} particles in the urban air of a town situated close to a steel works, *Atmos Environ* 2003;37:1013–22.
- Pancras JP, Landis MS. Performance evaluation of modified Semi-continuous Elements in Aerosol Sampler-III. *Atmos Environ* 2011;45:6751–59.
- Pancras JP, Ondov JM, Poor N, Landis MS, Stevens RK. Identification of sources and estimation of emission profiles from highly time-resolved pollutant measurements in Tampa, FL. *Atmos Environ* 2006;40:467–81.

- Pancras JP, Vedantham R, Landis MS, Norris GA, Ondov JM. Application of EPA Unmix and nonparametric wind regression on high time resolution trace elements and speciated mercury in Tampa aerosol. *Environ Sci Technol* 2011;45:3511–18.
- Pere-Trepat E, Kim E, Paatero P, Hopke PK. Source apportionment of time and size-resolved ambient particulate matter measured with a rotating DRUM impactor. *Atmos Environ* 2007;41:5921–33.
- Polissar AV, Hopke PK, Paatero P, Malm WC, Sisler JF. Atmospheric aerosol over Alaska 2. elemental composition and sources. *J Geophys Res* 1998;103:19045–57.
- Reff A, Eberly SI, Bhave PV. Receptor modeling of ambient particulate matter data using Positive Matrix Factorization: review of existing methods. *J Air Waste Manage Assoc* 2007;57:146–54.
- Seinfeld, J. H., Pandis, S. N. *Atmospheric Chemistry and Physics: From Air Pollution to Climate Change*; Wiley InterScience, 1998
- Talebi, SM, Abedi, M. Determination of arsenic in air particulates and diesel exhaust particulates by spectrophotometry. *Journal of Environmental Sciences*, 2005; 17 (1): 156-158.
- Turpin BJ, Lim HJ. Species contributions to PM_{2.5} mass concentrations: revisiting common assumptions for estimating organic mass, *Aerosol Sci Technol* 2001;35: 602–10.
- Thurston, G.D., Spengler, J.D. A quantitative assessment of source contributions to inhalable particulate matter pollution in metropolitan Boston. *Atmos. Environ.* 1985;19 (1): 9–25.
- U.S. EPA. Mercury Study Report to Congress, EPA-452/R-97-005, Office of Air Quality Planning and Standards, Office of Research and Development, Washington, DC, 1997.
- U.S. EPA. *EPA Unmix 6.0 Fundamentals & User Guide*. U.S. Environmental Protection Agency, Office of Research and Development, Washington, DC, 2007.

- U.S. EPA. The green book nonattainment areas for criteria pollutants, 2011a, <http://www.epa.gov/oaqps001/greenbk/>, last accessed February 9, 2012.
- U.S. EPA. *EPA Positive Matrix Factorization (PMF) 4.2 Fundamentals & User Guide*. U.S. Environmental Protection Agency, Office of Research and Development, Washington, DC, 2011b.
- U.S. EPA. National Emissions Standards for Hazardous Air Pollutants: Industrial, Commercial, and Institutional Boilers and Process Heaters, EPA-HQ-OAR-2002-0058, 2011c, <http://www.epa.gov/ttn/atw/boiler/boilerpg.html>, last accessed February 9, 2012.
- Vedantham R, Norris G, Brown SG, Roberts P. Combining continuous near-road monitoring and inverse modeling to isolate the effect of highway expansion on a school in Las Vegas. *Atmos Pollut Res* 2012;3:105–11.
- Wade KS, Turner JR, Brown SG, Garlock J, Hafner HR. Data Analysis and Source Apportionment of PM_{2.5} in Selected Midwestern Cities, Final Report STI-907018.03-3264-DFR, Prepared for Lake Michigan Air Directors Consortium, Sonoma Technology, Inc., 2008.
- Wichmann HE, Spix C, Tuch T, Wolke G, Peters A, Heinrich J, Kreyling WG, Heyder J. Daily mortality and fine and ultrafine particles in Erfurt, Germany. Part 1: role of particle number and particle mass, Research Report 98. Health Effects Institute, Cambridge, MA. 2000.
- Williams R, Brook R, Bard R, Conner T, Shin H, Burnett R. Impact of personal and ambient-level exposures to nitrogen dioxide and particulate matter on cardiovascular function. *Int J Environ Health Res* 2012;22:71–91.

Table 1. Species, method detection limits, uncertainty estimates, and hourly average compositions of the PM_{2.5} (n = 639)

Species	Measurement unit	MDL	Uncertainty estimate, %^a	Average conc.	One sigma
PM _{2.5}	µg m ⁻³	1	30	15.66	9.06
OC	µg m ⁻³	1.9	20	4.80	1.95
EC	µg m ⁻³	0.1	20	0.70	0.57
sulfate	µg m ⁻³	0.15	30	3.69	3.37
Nitrate	µg m ⁻³	0.1	30	0.81	0.98
Al	ng m ⁻³	5.6	26	14.95	19.59
As	ng m ⁻³	0.07	11	0.94	0.76
Ba	ng m ⁻³	0.79	25	3.45	2.54
Ca	ng m ⁻³	15.05	25	110.05	125.06
Cd	ng m ⁻³	0.04	30	0.30	0.81
Ce	ng m ⁻³	0.03	24	0.06	0.16
Cu	ng m ⁻³	1.23	28	3.08	3.38
Fe	ng m ⁻³	12.09	31	37.55	58.95
K	ng m ⁻³	3.81	26	70.10	94.88
La	ng m ⁻³	0.02	27	0.07	0.20
Mg	ng m ⁻³	5.42	24	25.71	42.19
Mn	ng m ⁻³	0.32	21	6.70	12.52
Na	ng m ⁻³	6.61	36	44.93	49.12
Ni	ng m ⁻³	0.2	40	0.36	0.54
P	ng m ⁻³	0.61	40	3.01	3.08
Pb	ng m ⁻³	0.78	33	4.04	5.74
Rb	ng m ⁻³	0.01	34	0.41	0.95
Se	ng m ⁻³	0.05	14	1.72	2.07
Sr	ng m ⁻³	0.11	26	1.15	1.63
Ti	ng m ⁻³	0.23	22	0.61	0.51
V	ng m ⁻³	0.02	14	1.03	1.85
Zn	ng m ⁻³	2.09	29	34.53	55.87

^aCollocated uncertainty estimate (Pancras and Landis, 2011).

Table 2. Dynamic variations in the concentration of hazardous air pollutants in Dearborn, MI, between July 13 and August 13, 2007.

Pollutant ^a	Unit	Concentration ^b Range	Percentile Concentration Range ^b				
			5th	25th	50th	75th	95th
As	ng m ⁻³	(BDL – 11.27)	0.12	0.38	0.73	1.28	2.56
Cd	ng m ⁻³	(BDL – 12.67)	BDL	BDL	0.08	0.23	1.39
Co	ng m ⁻³	(BDL – 0.53)	BDL	BDL	BDL	BDL	0.03
Mn	ng m ⁻³	(BDL – 129.35)	0.51	1.22	2.40	5.21	33.52
Ni	ng m ⁻³	(BDL – 23.11)	BDL	BDL	0.19	0.41	1.36
Pb	ng m ⁻³	(BDL – 80.57)	BDL	1.02	2.38	4.94	12.94
Sb	ng m ⁻³	(BDL – 10.53)	BDL	0.20	0.38	0.61	1.74
Se	ng m ⁻³	(BDL – 16.54)	BDL	0.29	0.98	2.31	5.73
GEM	ng m ⁻³	(1.30 – 12.60)	1.46	1.70	1.93	2.37	4.24
RGM	pg m ⁻³	(BDL – 183.28)	BDL	BDL	9.66	20.55	56.27
Hg(p)	pg m ⁻³	(BDL – 665.04)	BDL	5.17	7.56	10.39	23.57

^aTotal of 1450 30-min concentration measurements of As, Cd, Co, Mn, Ni, Pb, Sb, Pb, and Se; 669 hourly averages from 5-min measurements of gaseous elemental mercury (GEM); and 669 hourly measurements of divalent reactive gaseous mercury (RGM), and particulate bound mercury (Hg(p)) data were used to construct this table.

^bBDL denotes concentration below detection limit concentration.

Table 3. Linear regression analysis between Unmix and PMF (y/x) factor contribution estimates.

Unmix Factor (y)	PMF factor (x)	Slope	r ²	Intercept
Incineration	Incineration	1.03	0.59	-0.03
Secondary Nitrate/Selenium	Secondary Nitrate	0.76	0.57	0.24
Oil Combustion	Oil Combustion	0.92	0.99	0.08
Sinter/Slag Process	Sinter/Slag Process	0.88	0.98	0.12
Iron and Steel	Iron and Steel	0.50	0.55	0.50
Refinery (FCC)	Refinery (FCC)	0.88	0.99	0.12
Secondary Sulfate	Secondary Sulfate	0.77	0.73	0.23
Motor Vehicle	Motor Vehicle	0.14	0.07	0.86
Crustal/Road Dust	Crustal/Road Dust	0.79	0.30	0.18
Coal/Coke	Coal/Coke	0.71	0.53	0.29

Table 4. PM_{2.5} mass apportioned to various sources and similar literature findings in Dearborn, MI.

Sources/Source Types	Previous Studies ($\mu\text{g m}^{-3}$)				Current Study ($\mu\text{g m}^{-3}$)			
	Wade	Gildemeister	Brown	Hammond	PMF ^a		Unmix ^a	
Mobile Sources								
Gasoline	2.08	3.75	3.96	4.24				
Diesel	2.84	1.17	1.06	2.16				
Mobile source					1.27	(0.15 – 2.24)	4.42	(3.24 – 6.14)
Secondary Sources								
Secondary sulfate	5.24	4.84	4.49	10.89	6.89	(3.90 – 8.60)	5.85	(3.89 – 7.62)
Secondary nitrate	3.36	3.89	4.26		1.61	(0.89 – 3.98)	3.61	(2.23 – 4.88)
Industrial Sources								
Iron/steel manufacturing	1.27	1.24	0.81	0.75	0.36	(0.00 – 0.91)	2.14	(1.31 – 2.60)
Mixed industry/zinc	1.51	1.3	0.32	0.03				
Mixed industry/lead	0.55							
Municipal sludge incinerator					0.24	(0.05 – 0.96)	0.11	(0.00 – 0.52)
Oil refinery					0.00	(0.00 – 0.19)	0.00	(0.00 – 0.23)
Oil combustion				0.06	0.56	(0.12 – 1.10)	0.48	(0.11 – 0.91)
Slag/sinter processing					0.74	(0.22 – 0.85)	0.00	(0.00 – 0.17)
Biomass burning			0.31					
Coal combustion					0.06	(0.00 – 0.86)	0.00	(0.00 – 0.65)
Road Dust/Crustal	1.36	2.14	0.88	0.02	1.99	(0.57 – 6.08)	0.00	(0.00 – 0.50)
Sea Salt		0.72						

^a5th and 95th percentile concentrations from bootstrap analysis.

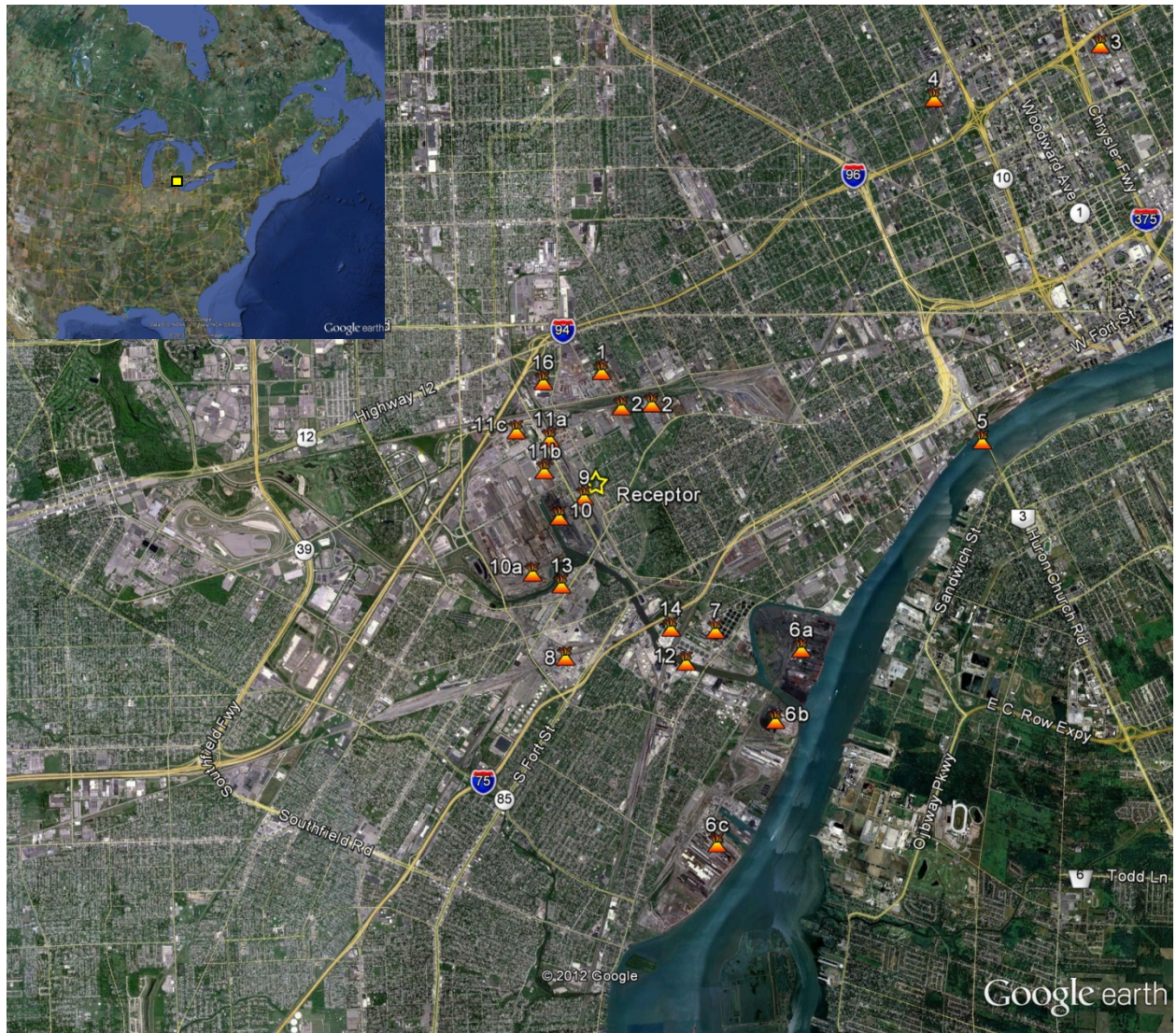


Fig. 1. Receptor location and industrial operations within 10 km radius. Sources are numbered: 1,4, and 16 – metals recycling and recovery; 2 – slag processing; 3 – municipal waste incinerator; 5 – ambassador bridge; 6a – metallurgical coke production; 6b & 6c – iron and steel manufacturing; 7 – municipal sewage sludge incineration; 8 – oil refining; 9 – commercial electric generation; 10 – iron and steel manufacturing; 10a – waste oxides reclamation facility; 11a, b, c – auto manufacturing; 12 – lime production; 13 – asphalt production; and 14 – gypsum production.

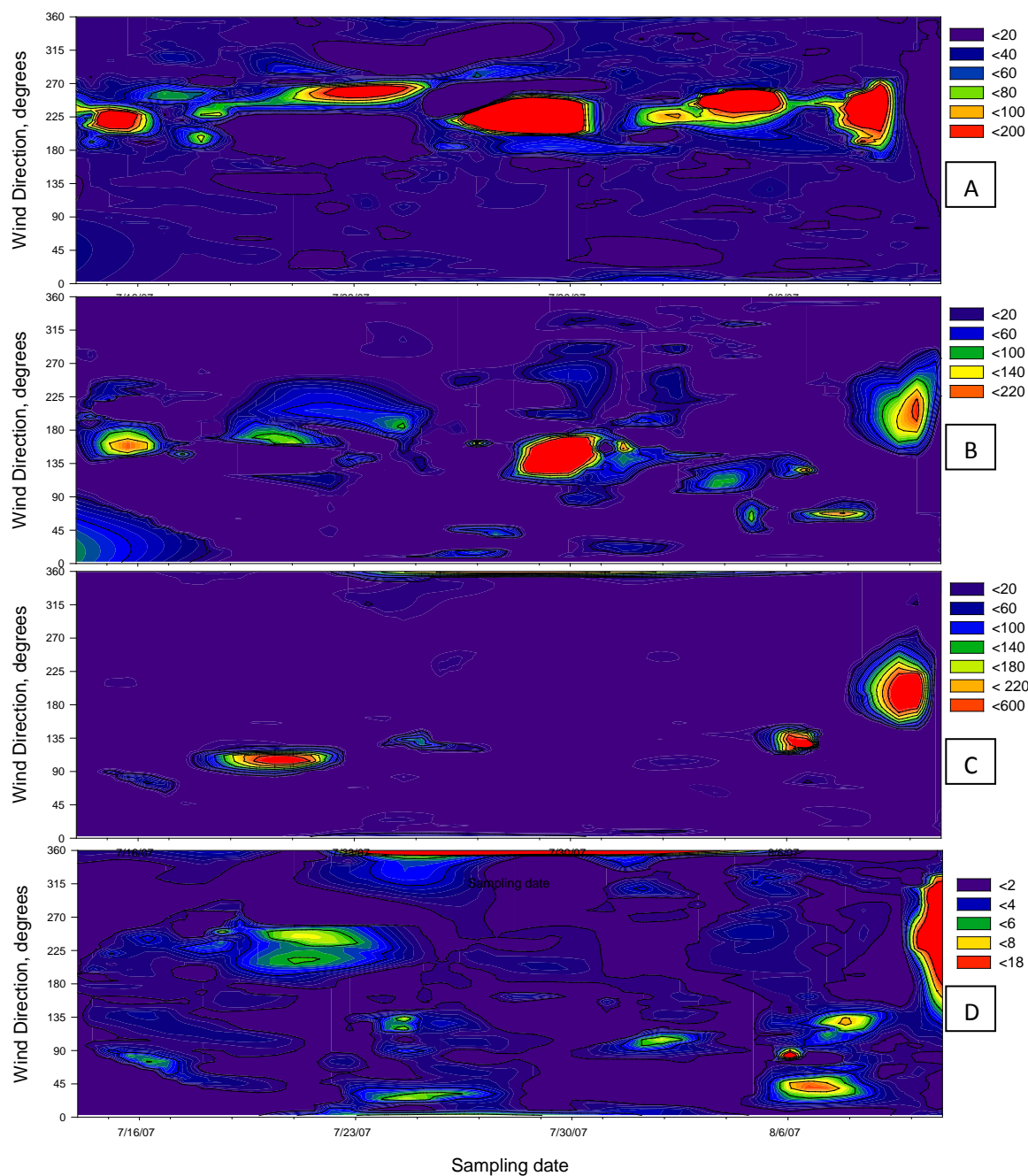
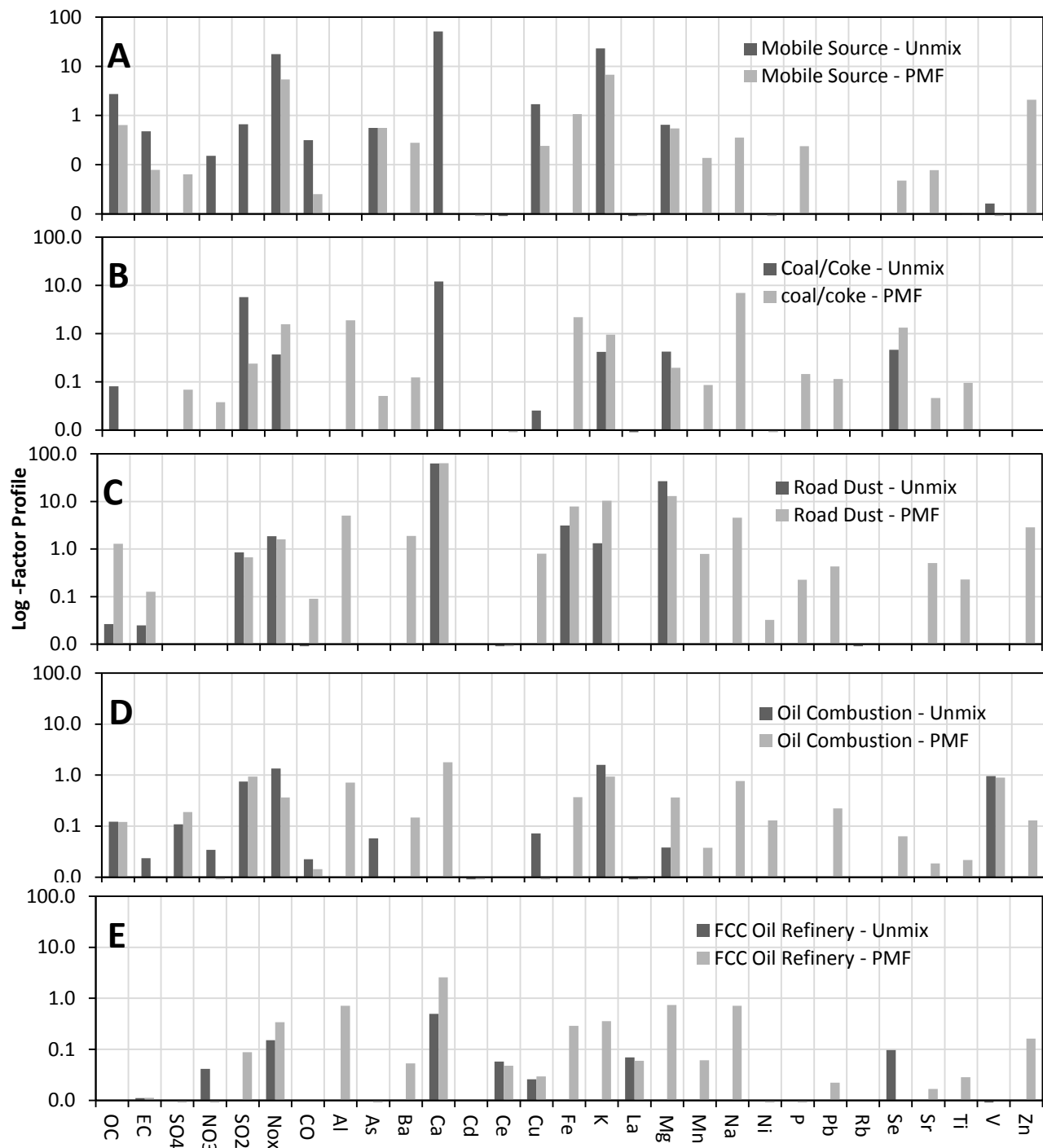


Fig. 2. 3D contour plots showing measured species concentrations at hourly resolution as a function of sampling time and surface wind direction: A – Mn, B – divalent reactive gaseous mercury (RGM), C – particle bound mercury (Hg(p)), and D – gaseous elemental mercury (GEM). Red and yellow areas indicate observed higher concentrations attributable to wind direction (y axis). Legend units are ng m^{-3} for plots A and D and pg m^{-3} for plots B and C.



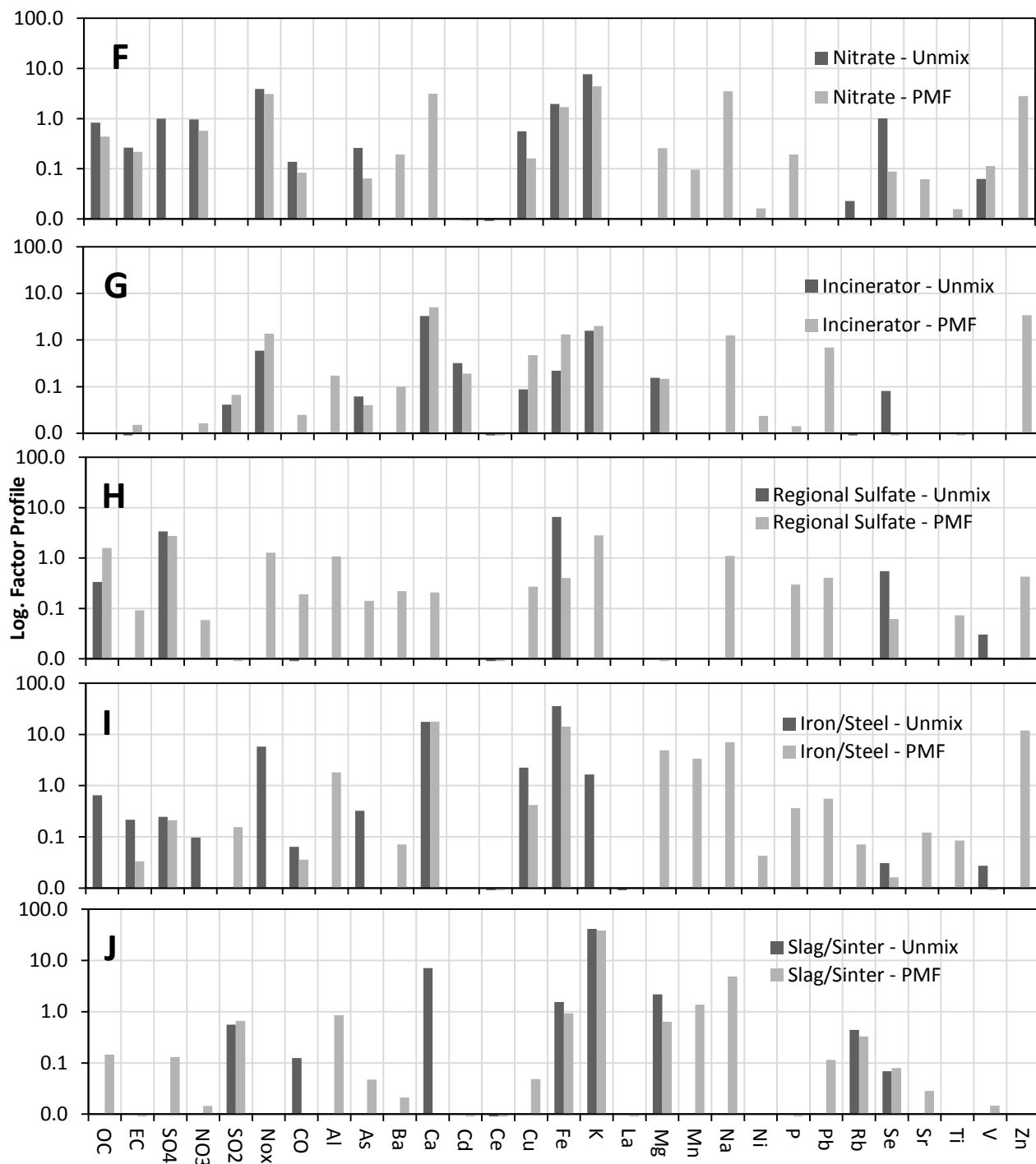


Fig. 3. Factor profiles from PMF and Unmix analysis. Profile units for species SO₂, NO_x, and CO are ppb; EC, OC, SO₄, NO₃ are $\mu\text{g m}^{-3}$; all other species are ng m^{-3} .

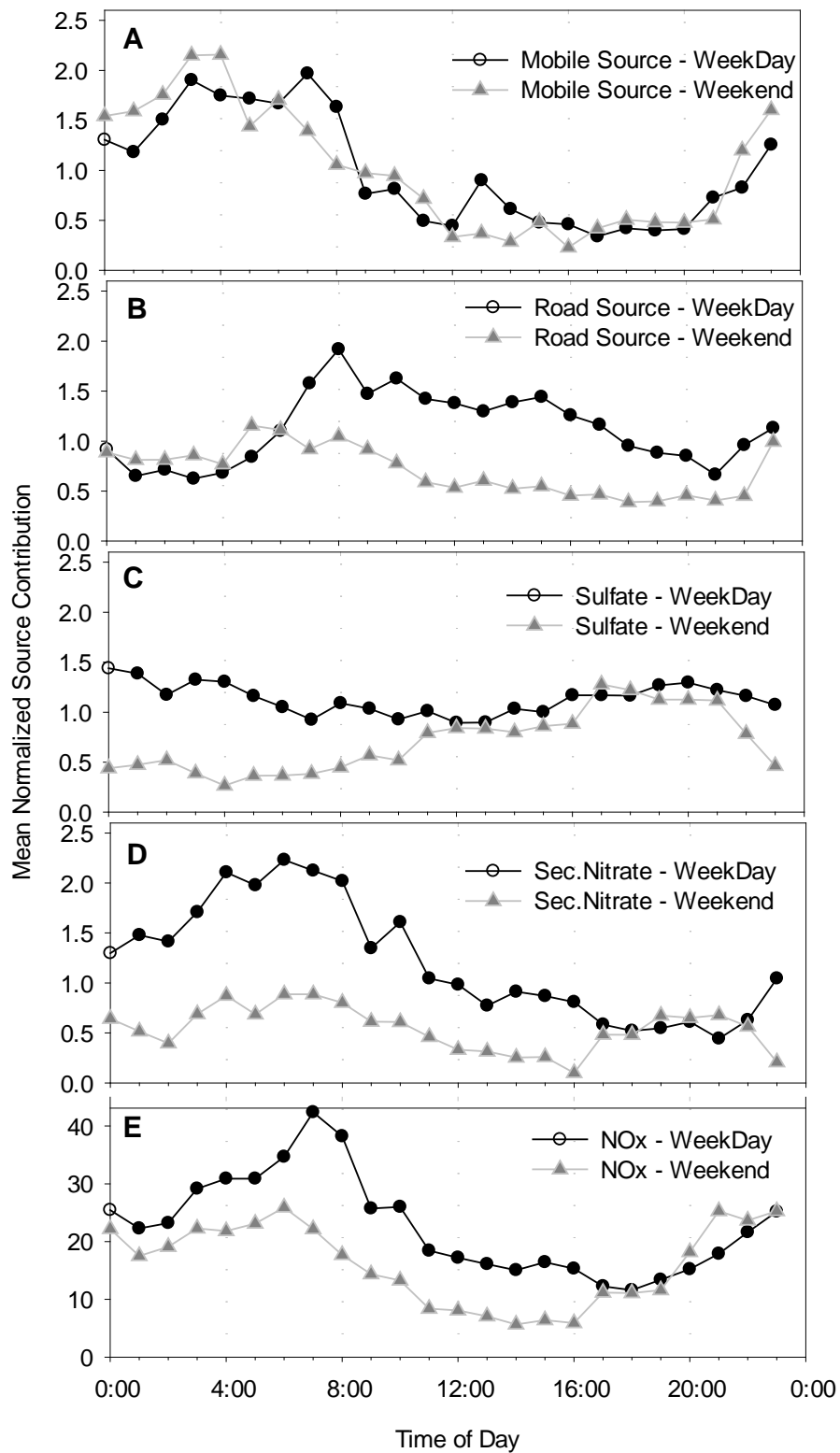


Fig. 4. Diurnal variations observed in the PMF model source contribution estimates (SCEs).

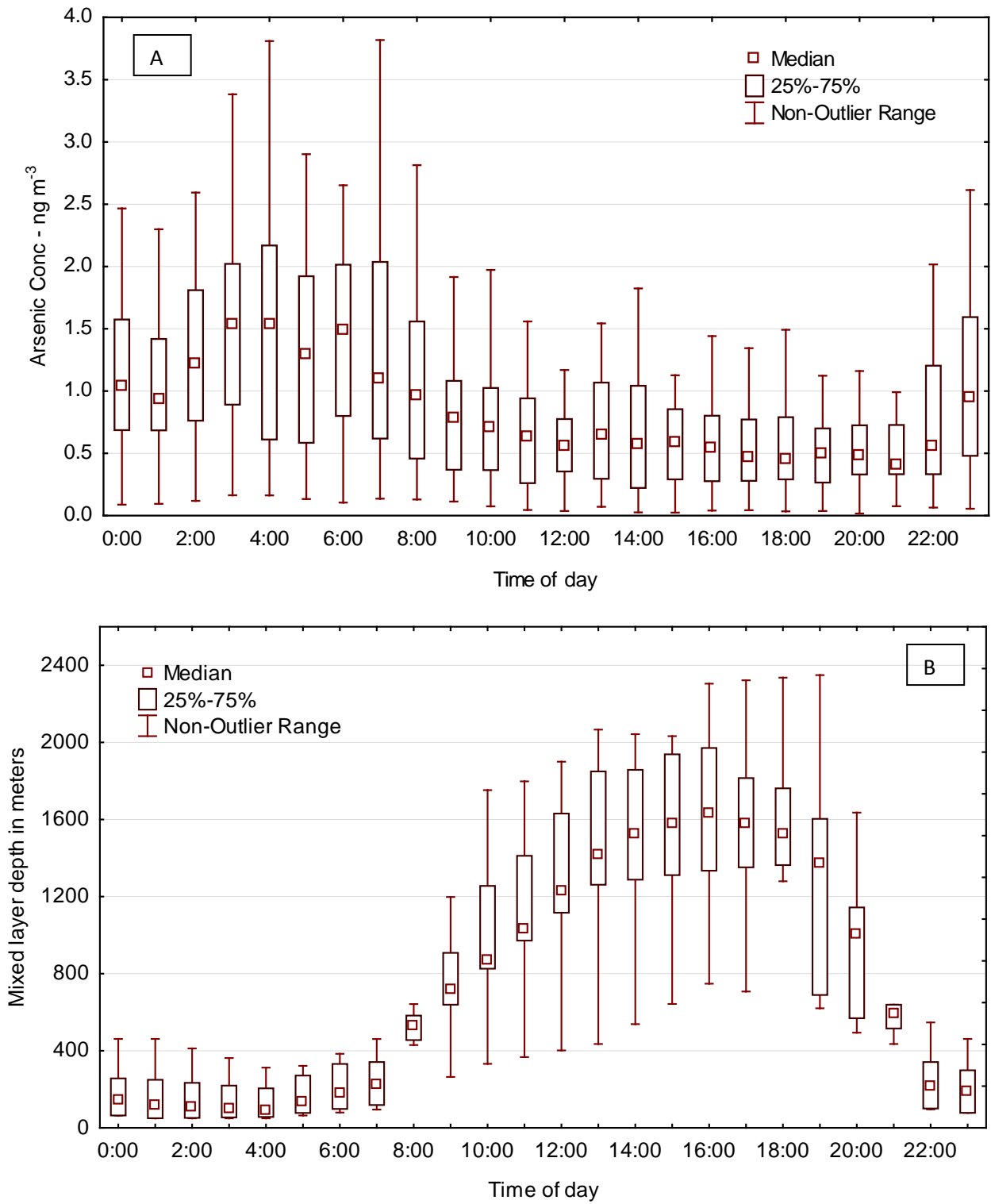


Fig. 5. Box plots showing (a) measured arsenic concentrations (ng m⁻³), and (b) boundary layer mixing height (m).

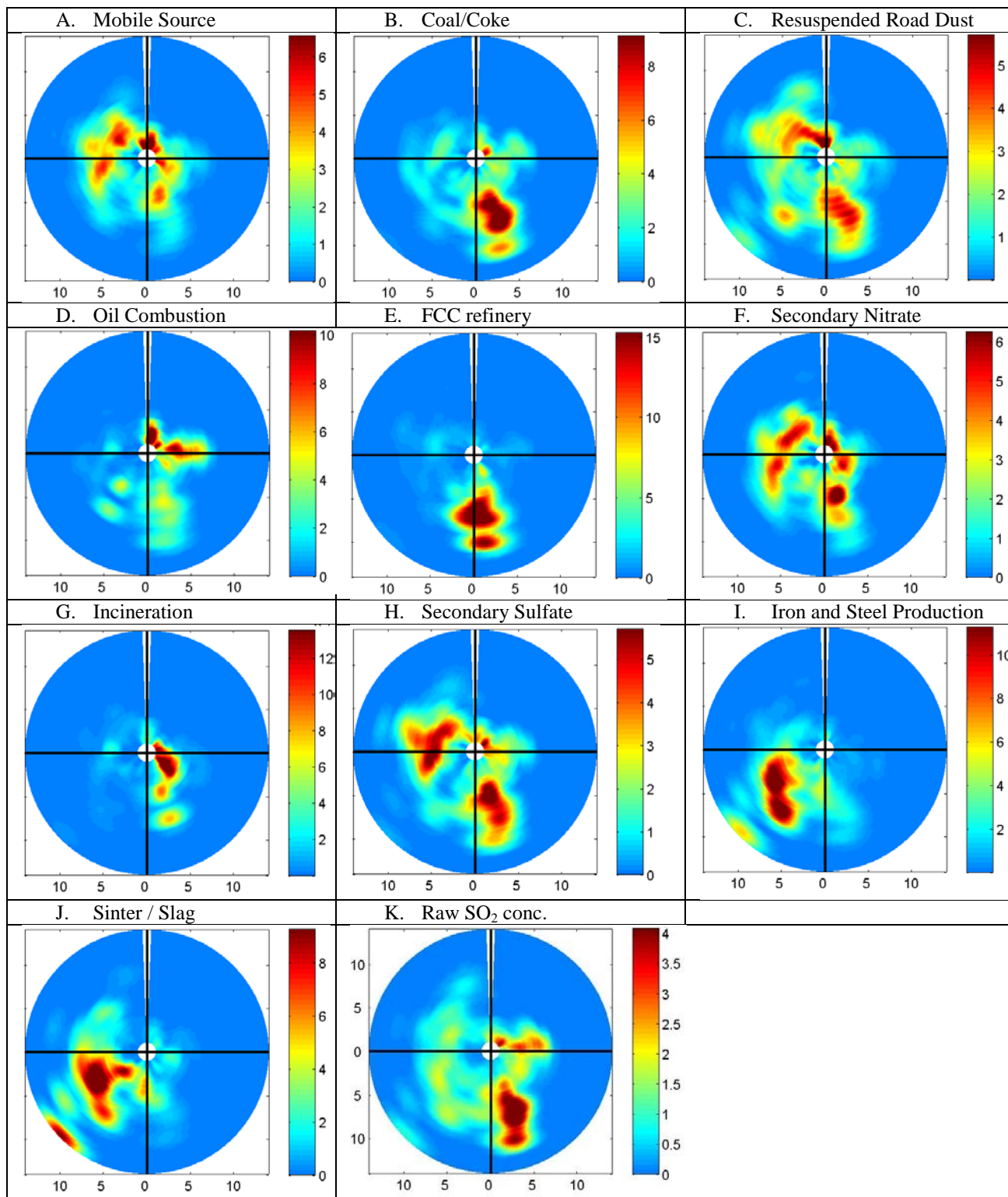


Fig. 6. SWIM plots depicting PMF model source contribution estimates (SCEs) spatial probability. Areas shown in red are high probability locations for the sources. The vertical and

horizontal axis represents wind speeds (m s^{-1}) associated with events from various directions. The color gradients represent SCEs values (A-J) and SO_2 concentrations (ppb; K).